OFFICE OF NAVAL RESEARCH

FINAL REPORT

PUBLICATIONS/PATENTS/PRESENTATIONS/HONORS/STUDENTS REPORT

for

Agreement Number: N00014-98-3-0020

PR Number 98PR07011-00

MEMS - Frequency Agile High Precision Ranging under the Dual Use Applications Program (DUAP)

Paul Bauhahn

Honeywell Laboratories

Communications Systems and Architecture

3660 Technology Dr.

Minneapolis, Minnesota 55418

4 December 2001

Final Report

Agreement Number	N00014-98-3-0020
Agreement Title	MEMS - Frequency Agile High Precision Ranging under the Dual Use Applications Program (DUAP)
Program Officer	James M. Short
Principal Investigator	Paul Bauhahn
Address	3660 Technology Dr.
City	Minneapolis
State	MN
Zip Code	55418
Phone No.	(612) 951-7844
FAX No.	(612) 951-7438
E-mail	paul.e.bauhahn@honeywell.com

TABLE OF CONTENTS

FINAL REPORT **2**

1.0 ABSTRACT **4**

2.0 INTRODUCTION **5**

2.1 TASK OBJECTIVE 5
2.2 TECHNICAL APPROACH 5

3.0 PRECISION RANGING SENSOR DESIGN **7**

3.1 OVERVIEW 7
3.2 PRECISION RANGING SENSOR SYSTEM DESIGN CALCULATIONS 8
3.3 ASIC DESIGN APPROACH 9
3.4 ASIC CIRCUITS 10
3.4.1 Random pulse generator *11*
3.4.2 Synchronization circuit *11*
3.4.3 Transmitter/impulse amplifier *12*
3.4.4 Impulse integrating receiver *12*
3.5 SIMULATED AND MEASURED SENSOR CHARACTERISTICS 14
3.6 ANTENNA SURVEY AND SIZE LIMITATIONS 16

5.0 TECHNICAL CONCLUSIONS AND ASSESSMENT **19**

6.0 TECHNICAL RECOMMENDATIONS **20**

7.0 REFERENCES **20**

1.0 Abstract

The objective of this program was laboratory demonstration of a low cost, jamming resistant, precision ranging system (radar) for proximity fuze and short-range measurement systems. Two approaches were envisioned: (1) The baseline—a baseband system directly radiating and detecting a random sequence of short pulses and (2) A higher risk design based on a transmitter using high-speed modulation of a micro-electromechanical (MEM) oscillator to avoid low frequency antenna radiation requirements. Size constraints drive the design toward small, single-chip monocycle pulse radar implemented in CMOS. This device with two external capacitors, a battery and a miniature antenna for the baseline approach is described in Figure 1-1. Triggering ranges from several inches to more than 6feet were demonstrated. Fabrication of MEM components on gallium arsenide for the second approach will require additional work.

While CMOS technology is almost ideal for the long time-constant, multiple pulse integration circuits in the precision ranging receiver and most of the transmitter circuits, it is insufficient for submunition sensor final output amplifiers. The issue is the small size of the submunition antenna. Either step recovery diode circuit or higher performance output transistors are needed to generate the high frequency spectrum required for efficient radiation from these antennas. Using a 0.5-micron BiCMOS/SiGe process, recently available for prototyping at MOSIS,[1] all of the required CMOS and faster output devices could be implemented with trivial modifications of the existing circuits.

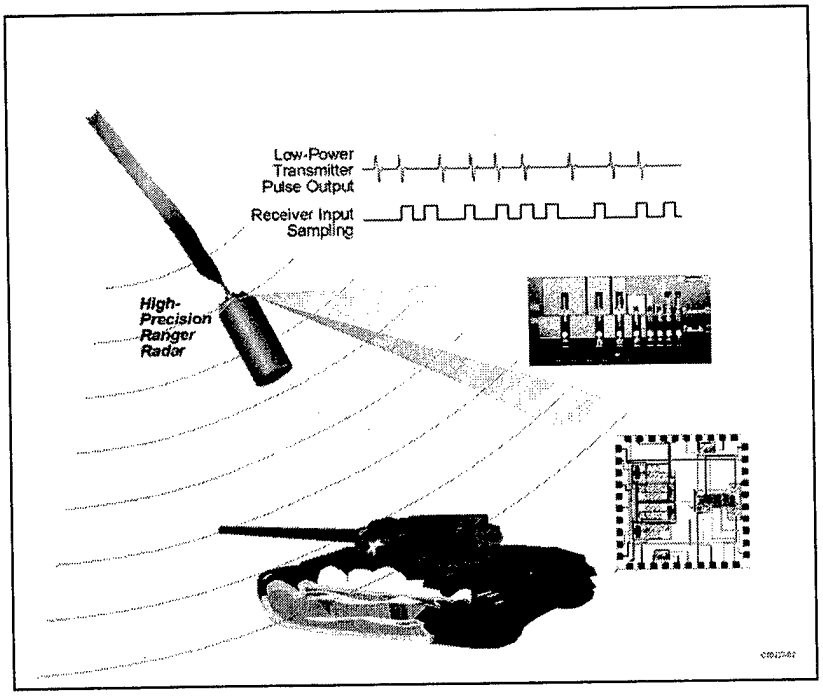

Figure 1-1 High precision single-chip radar using a RAKE receiver architecture with a random sequence of low power monocycles to measure target range

2.0 Introduction

2.1 Task objective

The program objective was development of short-range precision ranging sensors for both submunition and commercial applications. In the first application the size and power consumption are limited by the small size of the submunition. For the second, low cost and flexible ranges are important. Both applications can be addressed by integrating a complete short-range radar system on a single ASIC.

2.2 Technical approach

Good transmitter-receiver isolation is important for almost any radar system and is most easily achieved using pulse operation. For a one-foot range the total time available for the transmitted pulse and signal propagation to and from the target is less than 2 nanoseconds. In the baseline design this issue is addressed by reflecting of a subnanosecond monocycle from the target and using a receiver, synchronized to the transmitter, to sample the returned signal after a range delay. This sample is a few hundred picoseconds long. To improve performance, thousands of monocycles are transmitted at pseudo-random times, each one sampled after a short delay and the results integrated as described in Figure 2.2-1. The output of the integrator is a measure of the correlation between the sampling signal and the returned pulses. The overall performance is similar to a RAKE receiver design with the most recent pulses having the heaviest weighting. Long integration time constants and high-isolation sampling switches make the system quite jamming resistant.

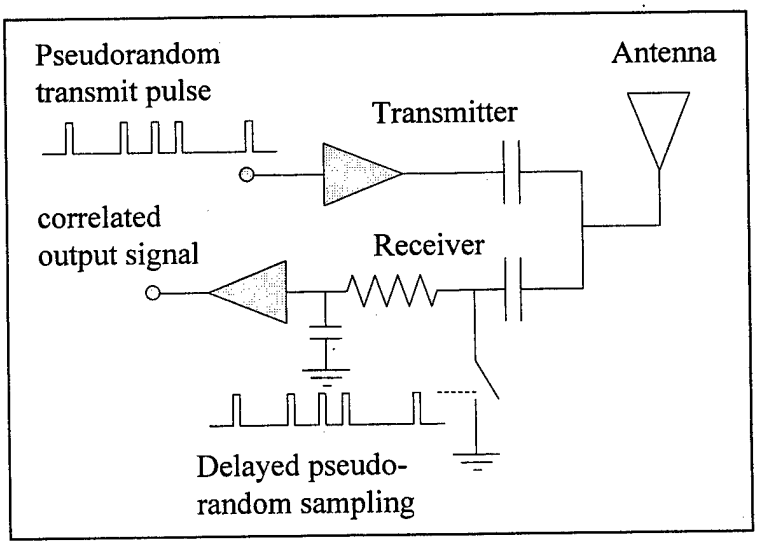

Figure 2.2-1 Simplified representation of the baseline precision ranging circuit and its operation

To use a very small submunition antenna the wide spectral bandwidth of the monocycle pulses should be moved to higher frequencies by employing faster rise and fall time pulses. At the same time, long time constants are required for pulse integration. Long time constants and low power consumption drives the design towards silicon CMOS circuits. Unfortunately, electrostatic discharge (ESD) protection circuits, pads and the antenna capacitance tend to degrade the transmitter performance with CMOS devices. A recently available high-speed silicon/ germanium BiCMOS process or a hybrid step recovery diode circuit could be used to for address this issue.

Rapidly modulating a microwave oscillator output can also be used to address submunition antenna size. The transmitted spectrum is then generated at higher frequencies. Ultimately this approach could be implemented with a silicon/germanium BiCMOS process. We originally proposed a hybrid design similar to the approach in Figure 5.1 for a preliminary demonstration.

3.0 Precision ranging sensor design

This section describes the architecture of the precision ranging sensor.

3.1 Overview

Short-range munition and measurement sensors have both size and cost constraints making designs based on a single integrated circuit especially attractive. The baseline ultra-short pulse radar ASIC in Figure 3.1-1 contains all of the required circuits for a submunition but an external microprocessor could be used for general purpose, short-range radar applications where more flexibility is required. Most of the area on the 2.2-mm x 2.2-mm ASIC is the result of the diagnostic pads and wouldn't be needed in production designs. Inspection of the layout indicates removing them could easily decrease the size and cost of the chip by at least a factor of two. There are other components required for complete sensors but even if the circuits were implemented in a somewhat more costly silicon-germanium process it would still result in a very economical device.

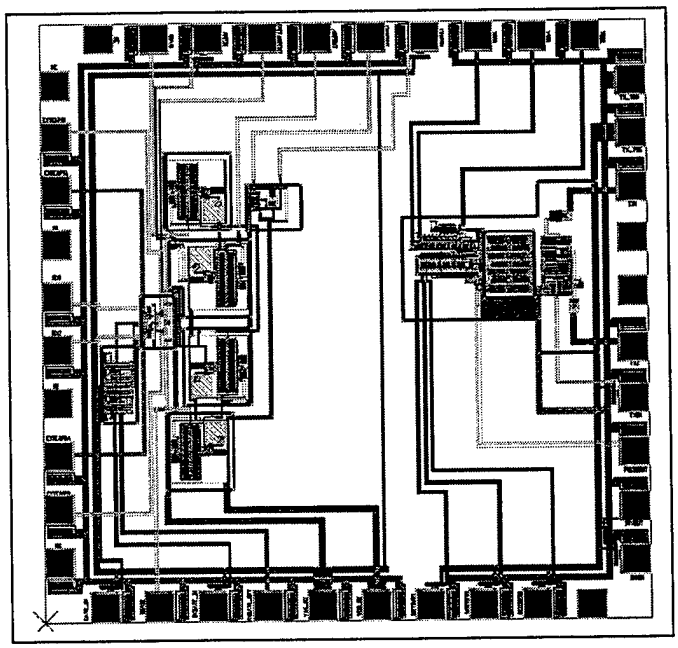

Figure 3.1-1 Ultra-short pulse 2.2-mm x 2.2-mm ASIC contains a complete radar sensor for low-cost munition and measurement applications

The remainder of this section will provide a more detailed discussion of the system and circuit design of the ASIC followed by a brief discussion of antenna development.

3.2 Precision Ranging Sensor System Design Calculations

The sensor range for a single pulse is calculated in Figure 3.2-1. While the assumptions are a bit optimistic the range should be more than adequate for sensor fuzed munitions transmitting multiple pulses.

$$BW = 2 \cdot GHz$$

$$P_n = 10 \cdot \log(k \cdot T \cdot B) + 10 \cdot dB = -71 \cdot dB$$

$$P_{rx} = P_n + 9.5 \cdot dB = -61.5 \cdot dB$$

$$P_{tx} = 1 \cdot mW$$

$$L = P_{tx} + G_{tx} + G_{rx} - FM - P_{rx} = 46.5 \cdot dB$$

$$\lambda = \frac{3 \cdot 10^{10} \cdot cm/\sec}{2 \cdot GHz} = 15 \cdot cm$$

$$D = \frac{\lambda}{4 \cdot \pi} \cdot 10^{\frac{L}{20}} = 2.5 \cdot m$$

Figure 3.2-1 Assuming a 10 dB receiver noise figure, requiring a 10^{-5} BER, a 1 mw transmitter output power P_{tx}, 0 dB antenna gains (G_{tx} and G_{rx}) and a 15 dB fade margin (FM) the calculated range is 2.5 meters

The wide transmitted spectrum is the primary source of inaccuracy in these calculations. Since antenna efficiency varies with wavelength they should just be regarded as feasibility estimates.

3.3 ASIC Design Approach

The most important constraints in designing the ASIC were the following, based on the anticipated applications:

- Design would use no off-chip components other than a couple capacitors, a battery and an antenna to fit in the small space available
- Less than 0.1 mA-hr battery capacity for munition applications
- Mask sharing prototype semiconductor fabrication process

The primary effects of the first constraint were elimination of all external time references and some degradation in the accuracy of the range measurements. In production, if improved timing accuracy were needed in a particular application, on-chip delay circuits could be trimmed or an external crystal employed.

The second constraint is important in controlling the battery size and the third reduces the cost of the ASIC development.

3.4 ASIC Circuits

The overall block diagram of the ASIC is in Figure 3.4-1 and a flow diagram describing its operation is in Figure 3.4-2. For the prototype the control inputs consist of bond wire connections to the power supply or ground. For submunition applications, these inputs could be eliminated. For more complex sensors, a low-cost external controller could be used.

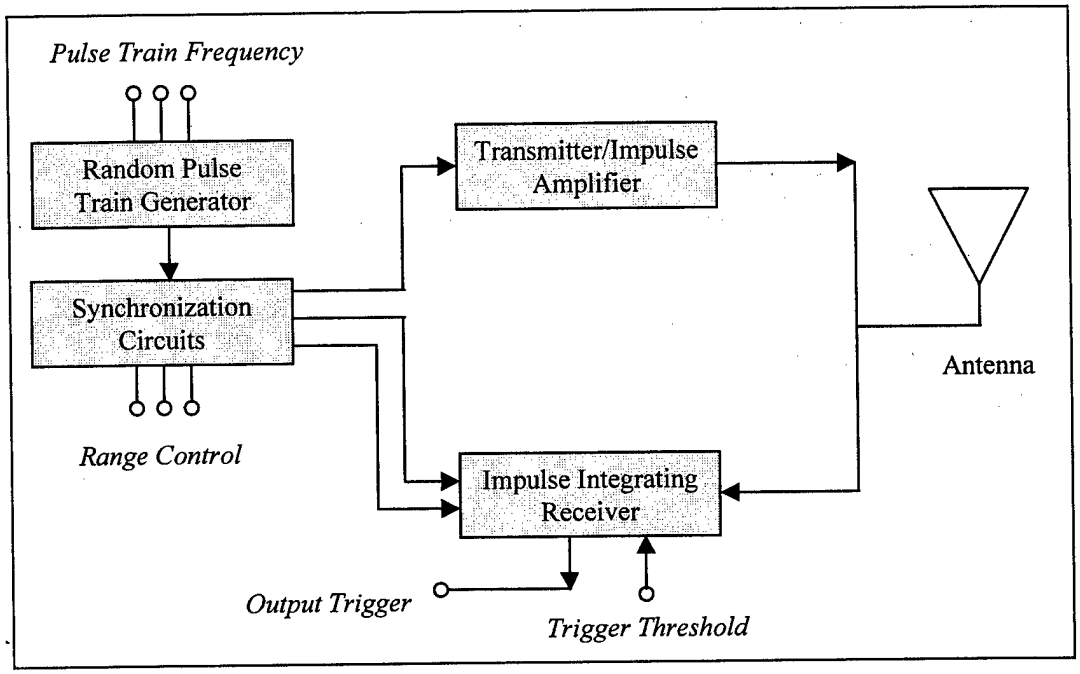

Figure 3.4-1 Overall baseline precision sensor block diagram

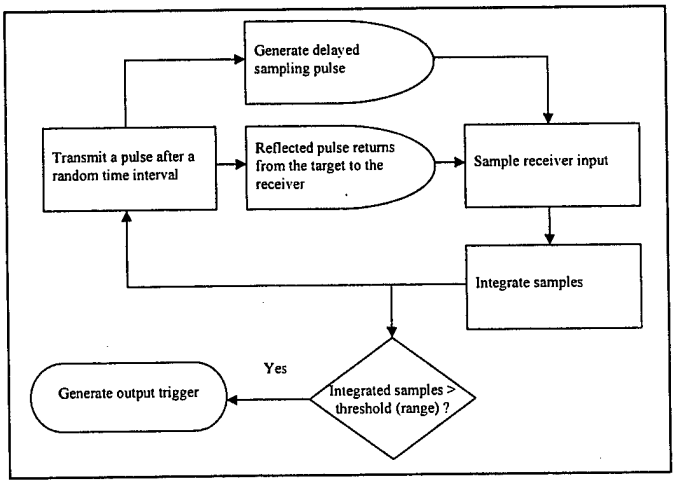

Figure 3.4-2 Sensor flow diagram describes ASIC operation

3.4.1 Random pulse generator

Figure 3.4-3 contains a simplified block diagram of the ASIC random pulse generator. To minimize circuit size the oscillators within the random pulse generator operate at frequencies greater than 100 MHz. Other oscillators modulate analog delays within these oscillators and the output is divided down to the lower repetition rates required for sensor operation. Three control inputs are employed to adjust the repetition rate to values appropriate for a particular range.

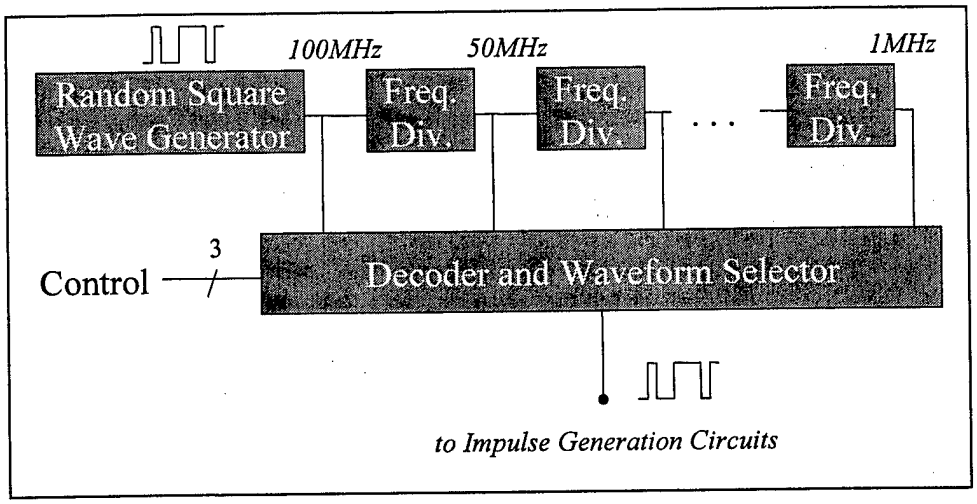

Figure 3.4-3 Simplified block diagram of the ASIC random pulse generator describes the control inputs used to select values appropriate for various ranges

3.4.2 Synchronization circuit

A block diagram for the sensor range gate is in Figure 3.4-4. By using the leading edge of a relatively low frequency, random pulse train to synchronize the impulse generators described in Figure 3.4-5 they could be placed close to the circuits requiring their outputs. This ASIC layout was less critical than one directly distributing the high frequency impulses around the chip.

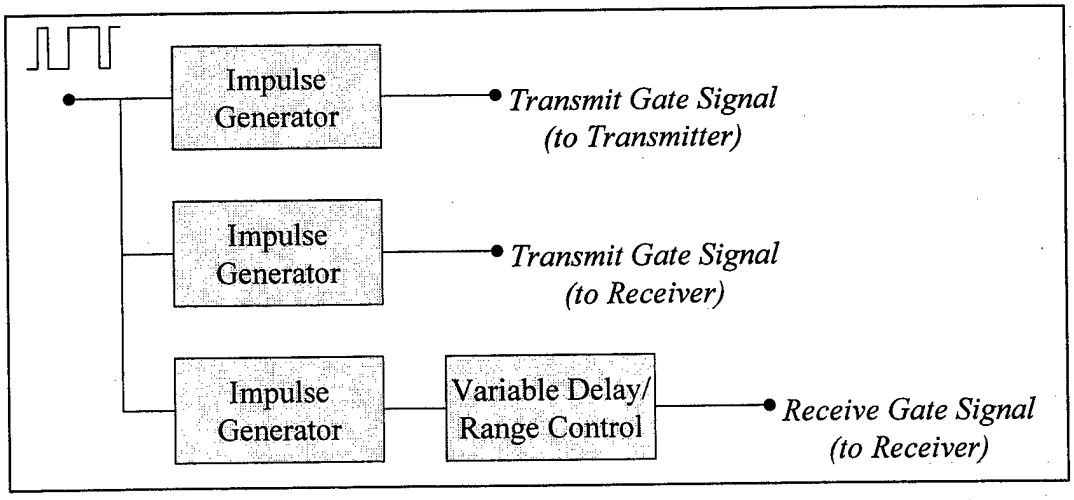

Figure 3.4-4 Circuit synchronizing the transmitter impulse output and the receiver isolation and sampling switch operations.

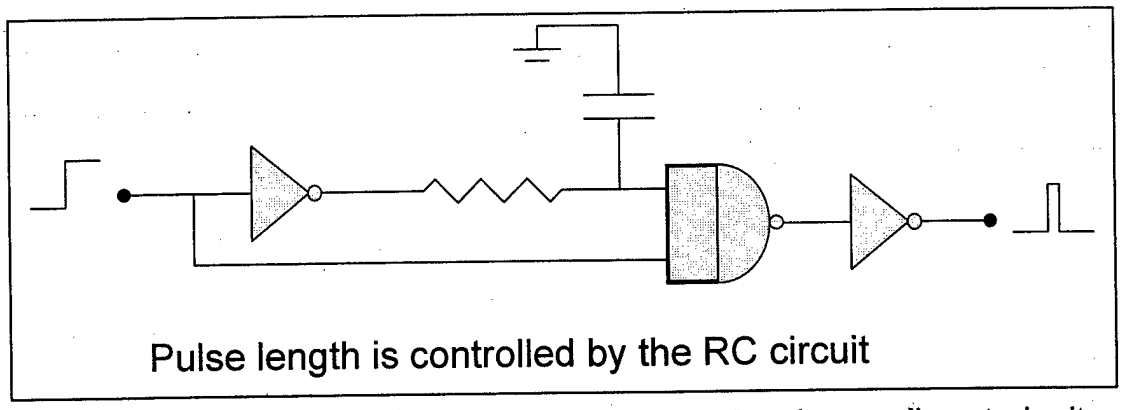

Figure 3.4-5 Impulse generator is a part of the transmitter and receiver sampling gate circuits

3.4.3 Transmitter/impulse amplifier

The transmitter impulse amplifier consists of a series of scaled-geometry inverter circuits as indicated in Figure 3.4-6. Except when changing state, these circuits consume little power. Two antennas are connected to complementary transmitter outputs in the figure but other configurations can be readily used without circuit modifications.

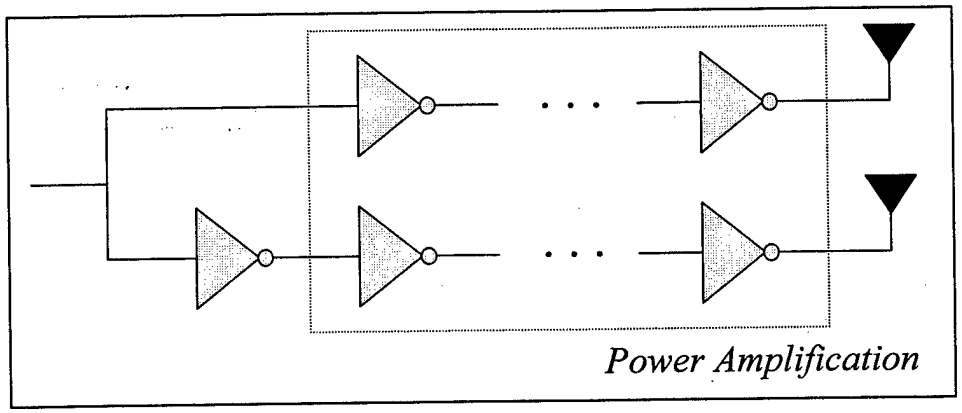

Figure3.4-6 Transmitter impulse amplifier contains a series of scaled-geometry inverter circuits.

3.4.4 Impulse integrating receiver

While many different receiver designs could be used, in this application the sampling pulse receiver in Figure 3.4-7 was employed. It has the advantage of being fairly simple and easily implemented in silicon CMOS technology. The mixer employs a balanced RF input, an active differential amplifier for the IF output and a single-ended LO/sampling signal input. The coupling capacitors integrate the received input pulses when the sampling switches are closed. For increased isolation the amplitude of the pulses applied to the receiver input are attenuated by opening a normally closed set of switches connected to the antenna during transmissions. Additional shunt switches (with inverted inputs) in the same position would provide additional isolation. This mixer design, while quite conventional, has some elements in common with the design discussed in Reference 2.

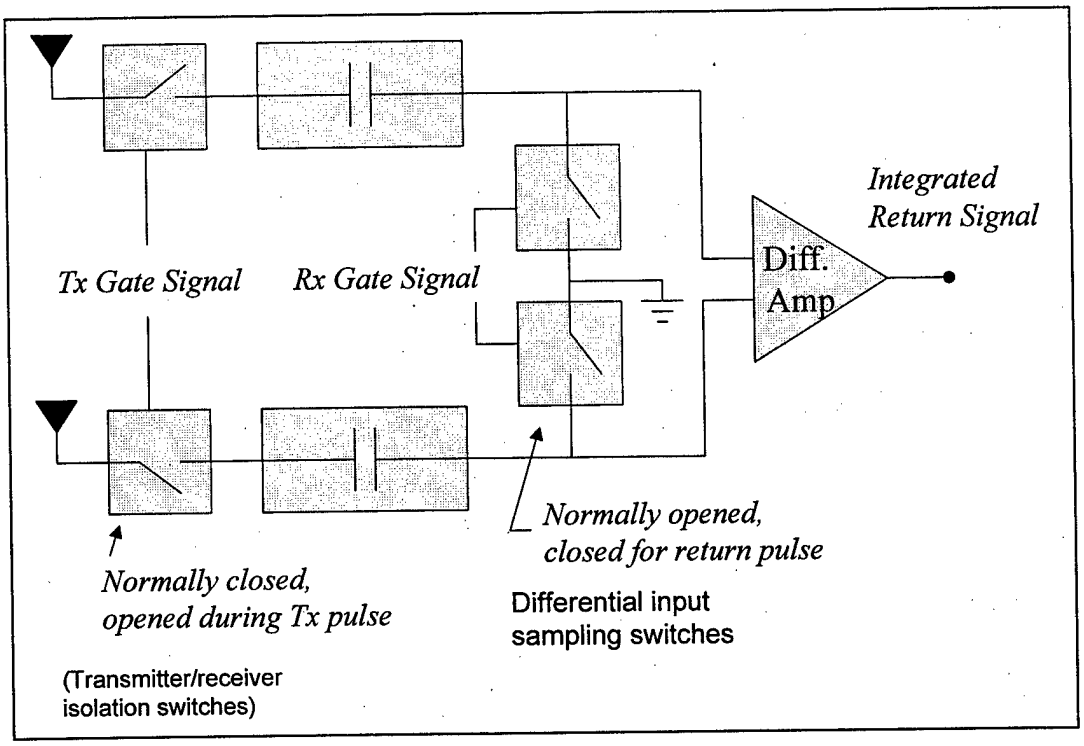

Figure 3.4-7 Block diagram of impulse integrating receiver containing transmitter isolation switches to improve signal-handling characteristics. This is a single-balanced mixer with a differential RF and IF input and output, respectively.

3.5 Simulated and measured sensor characteristics

The calculated difference between the two output terminals of the ASIC transmitter and its Fourier transform are in Figure 3.5-1. This approximates the signal applied to the terminals of a dipole antenna with a floating substrate.

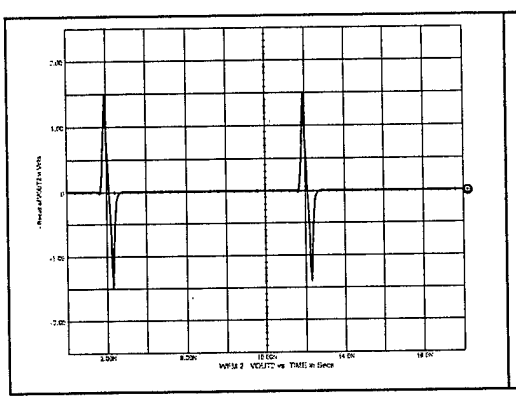

Figure 3.5-1a Simulated difference between transmitter output terminal voltages

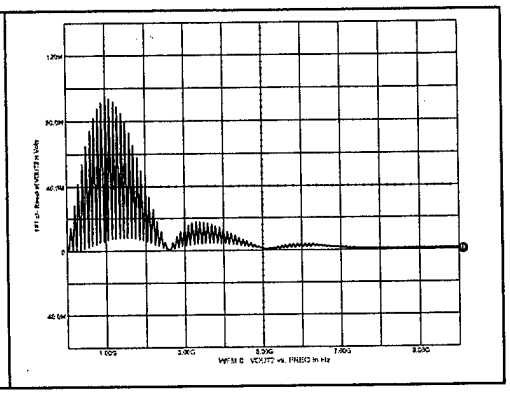

Figure 3.5-1b A Fourier transformation gives the frequency content

The measured outputs from the same two terminals, using directly connected instruments, are in Figure 3.5-2. There is some ringing but, generally, the response is quite similar. One would expect increased ringing when a small antenna terminates these outputs but the detrimental effects in this application should be relatively small since the system responds to the initial pulse. However, faster devices would be desirable in the transmitter circuits to decrease the pulse length providing an output spectrum more appropriate for small antennas.

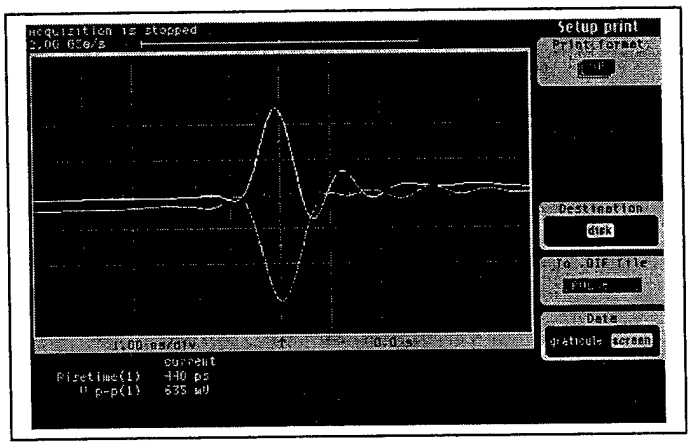

Figure 3.5-2 Measured output pulses at the transmitter terminals into 50-ohm loads are similar to the theoretical results

Figure 3.5-3 contains the measured correlation between the output of the transmitter and the returned signal as the delay is scanned. The high resolution of the receiver and transmitter jitter

(a simple ring oscillator was used for timing) is probably responsible for the maximum correlation being less than one.

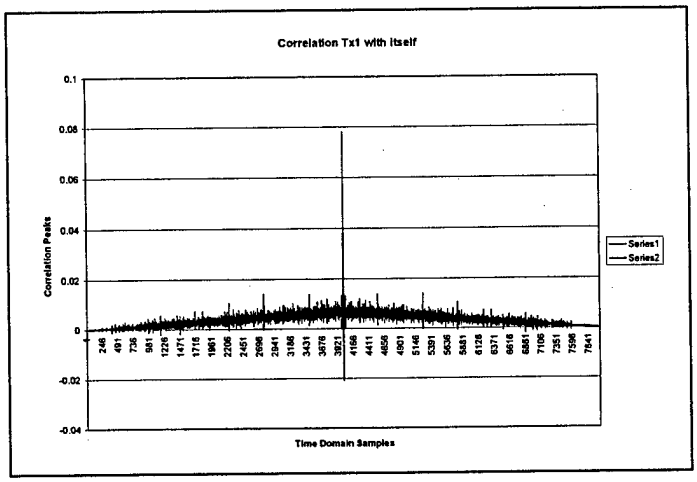

Figure 3.5-3 Correlation between the transmitter output and itself indicates relatively good security but further improvements are needed.

3.6 Antenna survey and size limitations

To address the issue of submunition size the matching characteristics and radiation efficiency of various antennas were evaluated. Limitations on the potential bandwidth of small omnidirectional antennas are calculated in Figure 4-1[3-5]. These results demonstrate the need for such an investigation. Since modern submunition dimensions are not much larger than a few inches there are three potential choices for satisfying antenna constraints for impulse radar in this application: (1) Antenna Q's smaller than unity or (2) Ultra-short pulses placing most of the radiated spectrum at higher microwave frequencies. (3) Employ the streamer or other wires extending from the housing as a part of the antenna. Based on the survey results reported in this section it appears that a modification of the cylindrical structures used for the submunition with appropriate radial ground wires can probably meet precision ranging requirements with some decrease in antenna efficiency.

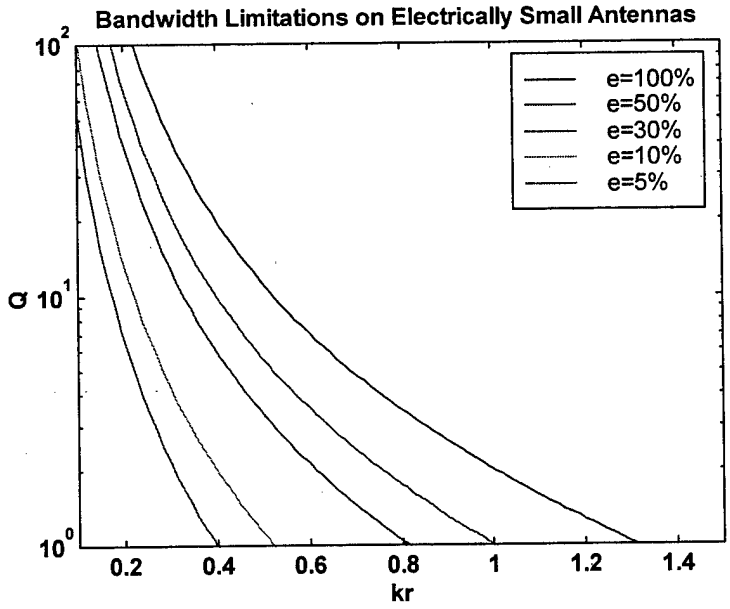

Figure 4-1 Theoretical calculation of omnidirectional antenna *Q* vs. *r*, the radius of an enclosing sphere, and the efficiency *e* emphasizes the limitations of small antennas for wide bandwidth operation.

For other applications the loaded disk also shows promise for reduced antenna size, wide bandwidth and good efficiency.

As mentioned previously, modified electronics could also be employed to place the output spectrum at higher frequencies to accommodate smaller antennas.

The measurements to be discussed were not made in an anechoic chamber so there were some multipath effects. The testing was just intended to obtain a qualitative look at various structures. Since radiation efficiency tests employed antennas with limited bandwidths, results are primarily useful for comparisons between antennas.

Antenna structures investigated:

- Quarter wave monopole
- Half wave dipole
- Disk
- Ring
- Ring with resistance
- Loaded disk
- Cylinder

The quarter wave monopole was used as a baseline design and for radiation efficiency measurements. A 12 inches square metal plate was employed to minimize ground plane effects.

A half-wave dipole having spiral tapered elements (width/length ratio = 0.4) was constructed and tested. Although it was not optimally matched it did show a considerable increase in radiated bandwidth, i.e., 75% vs. 43% for a conventional non tapered design, (diameter/length ratio = .038).

The disk antenna, 1" diameter, gave a very good match when used with a large ground plane. The radiated bandwidth was 80% and radiation efficiency was equal to a conventional dipole or monopole. The disk element structure provides a significant increase in bandwidth and about a 10% reduction in length compared to a wire element.

A ring antenna was constructed using .06" diameter wire wound in a one-turn coil, 1.44" diameter, and mounted on a ground plane. The radiated bandwidth was similar to the disk antenna. The VSWR was not as good, partially explaining the approximately 3dB higher loss. This implies the ring is about as good as the solid disk. Another variant of the ring left a gap, 0.06", where the wire coil comes back to the feed point. The performance of this structure was similar to the continuous coil.

Using the gapped ring antenna, a 50-ohm resistor was used to terminate the open end of the coil to ground. We hoped improving the low frequency match could extend the low frequency cutoff. Although the low frequency match was improved at very low frequencies, in the band of interest the VSWR improvement was minimal due to the coil inductance.

A 0.5" diameter copper disk was loaded with 0.1" thick Trans-Tech ceramic material, e_r=77, by sandwiching the disk between two ceramic pieces. Compared to the 1" diameter disk, the smaller disk had about 2-dB lower radiation efficiency while the bandwidth decreased from 80 to 68 percent. The loaded disk has about 2db higher loss with greater bandwidth and significantly smaller size than the full size dipole.

Experiments were also completed with a solid cylinder. The 1.25" diameter by 1.75" long copper cylinder was mounted on a large ground plane to measure its natural resonance. The cylinder resonated at 1.6 gigahertz and had a 10db return loss bandwidth of 1.2 gigahertz. It was then tested with various length ground wires replacing the 12" ground plane. The optimum

length was 1.9" when wire pairs were tested but additional wires would probably be helpful. With this configuration the VSWR bandwidth was better and radiation efficiency approximately 2 dB worse than the monopole and dipole over the frequency range of 1.0 to 2.4 gigahertz. This is probably one of the better candidates for wider bandwidth submunition antennas.

Operating the electronics at higher frequencies could reduce antenna percentage bandwidth requirements. Unfortunately, with the gallium arsenide-based MEMS processing for extending the performance of the precision ranging system to higher frequencies was unsuccessful. Figure 4-1 describes our preliminary approach for translating wide bandwidth modulation to higher frequencies. The primary tradeoff would be somewhat increased power consumption. Ultimately, all of these functions could be realized on the same chip.

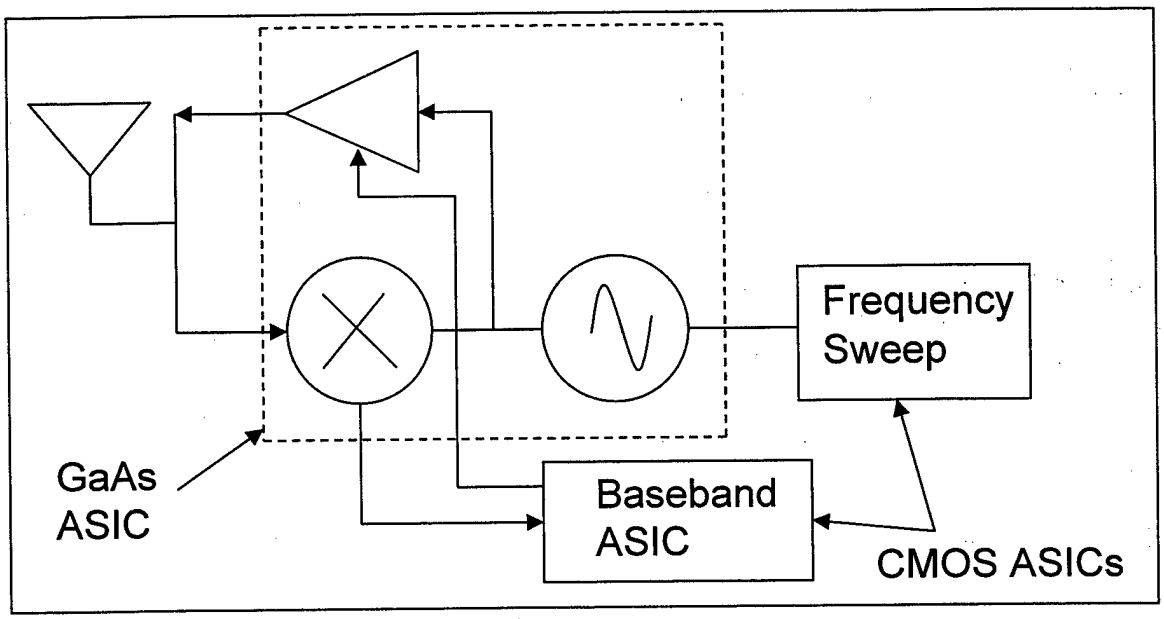

Figure 4-1 Proposed sensor extension to higher frequencies permitting smaller antennas

5.0 Technical conclusions and assessment

The baseline circuits developed in this program can be modified for a variety of applications with very little effort. The CMOS devices used are most appropriate for building the required complex low-power receiver circuits. For submunition applications the receivers need integration times on the order of milliseconds and operating frequencies less than 1 megahertz. Achieving these characteristics with crystal-controlled circuits isn't very difficult, but eliminating the crystal degrades the estimated range accuracy to about $\pm$20% if no trimming of on-chip resistors is employed. With trimming, the performance degradation from process variations can probably be improved to $\pm$5 or $\pm$10%.

Faster output devices are needed to generate the short, large amplitude transmitter pulses compatible with small submunition antennas. To minimize the sensor size these transmitter devices need to be integrated with the CMOS receiver. This capability is now available with recently introduced silicon-germanium processes providing both heterojunction bipolar transistors and CMOS devices. Other techniques for generating shorter transmitter pulses have been investigated but suffer from either excessive size (nonlinear transmission lines) or nonstandard semiconductor process requirements (step recovery diodes). The latter precludes realization of the complete sensor on a single, low power ASIC.

Improved isolation between the receiver and antenna are also desirable and easily achieved by adding a shunt transistor prior to the input capacitors. This would provide improved jamming resistance.

When FCC requirements are stabilized some adjustment of the waveforms will be needed to minimize interference with existing services such GPS radios. All of these issues can readily be addressed.

6.0 Technical recommendations

With rare exceptions recent FCC rulings require confining UWB radiation sources to the interior of buildings to avoid interference with other electronic systems. If an exception could be obtained for this application, we would recommend developing a precision single-chip UWB sensor based on many of the circuits devised for this program. Without such an exception further development in this area should be terminated.

7.0 References

1. http://www.mosis.com

2. Thomas E. McEwan, "Ultra-Wideband Receiver", US Patent 5,345,471.

3. H. A. Wheeler, "Fundamental Limitations of Small Antennas," Proc. IRE, pp. 1479-1488, December 1947.

4. L. J. Chu, "Physical Limitations on omni-direction antennas," J. Appl. Phys., vol. 19, pp. 1163-1175, December 1948.

5. R. C. Hansen, "Fundamental Limitations in Antennas," Proc. IEEE, vol. 69, No. 2, pp. 170-182, February 1981.